Proposed Model for Uniaxial Tensile Behavior of Ultra High Performance Concrete

Dr. Hisham M. Al-Hassani,
Building and Construction Engineering Department, University of Technology/ Baghdad.
Dr. Wasan I. Khalil
Building and Construction Engineering Department, University of Technology/ Baghdad.
Email: wasan1959@yahoo.com
Lubna S. Danha
Building and Construction Engineering Department, University of Technology/ Baghdad.

Received on: 22/7/2014 & Accepted on: 4/12/2014

ABSTRACT

This paper investigates experimentally the complete uniaxial tensile stress-strain relationships of Ultra high performance concrete (UHPC) and equations for expressing such relationships are obtained. The effects of two variable parameters on the uniaxial tensile behavior were carefully studied which are the silica fume content SF (0%, 10%, 15%, 20%, 25%, and 30%) as a partial replacement by weight of cement, steel fibers volume fraction V_f (0%, 1%, 2% and 3%). The experimental results showed that the two variables of the present investigation had no significant effect on the shape of the ascending part of the stress-strain curve, while the descending part of the curve was found to be considerably affected by the volume fraction V_f of the steel fibers used. Increasing fibers volume fraction V_f from 0% to 3% not only increase the area under the uniaxial tensile stress–strain curve, but also increase both the maximum uniaxial tensile strength by 238.5% and its corresponding strain by about 4044%. Two nonlinear equations are suggested in this research to model the ascending and descending part of the uniaxial tensile stress-strain relationship which are found suitable to represent the uniaxial tensile behavior of the UHPC mixes.

Keywords: Uniaxial Tensile stress-strain relationship, Steel fibers, Silica fumes.

نموذج مقترح لسلوك الشد المحوري للخرسانة المتفوقة الأداء

https://doi.org/10.30684/etj.33.1A.5
2412-0758/University of Technology-Iraq, Baghdad, Iraq

الخلاصة

يقدم هذا البحث تحري عملي للعلاقة المتكاملة بين الإجهاد والإنفعال في حالة الشد المحوري لخرسانة متفوقة الأداء, كما تم ايجاد معادلات للتعبير عن هذه العلاقات. تم بعناية دراسة ومناقشة تأثير متغيران, محتوى ابخرة السليكا المكثفة (0%, 10%, 15%, 20%, 25%, 30%) والنسبة الحجمية للالياف الفولاذية (0%, 1%, 2%, 3%). اظهرت النتائج العملية أن المتغيران للبحث الحالي لم يكن لهما تأثير كبير على شكل الجزء الصاعد من منحنى الإجهاد-الانفعال، في حين وجد أن الجزء النازل من المنحنى يتأثر بشكل كبير بتغير النسبة الحجمية للألياف الفولاذية المستخدمة . كما أظهرت النتائج أن زيادة نسبة الألياف الفولاذية من 0٪ إلى 3٪ لاتؤدي الى زيادة المساحة تحت منحنى إجهاد-انفعال الشد المحوري فحسب وانما تزيد أيضا كل من مقاومة الشد المحوري القصوى بحدود 238.5% والانفعال المصاحب لها بحوالي 4044%. و لقد وجد ان المعادلتين اللاخطية المقترحة لنمذجة الجزء الصاعد والنازل من منحني إجهاد-انفعال الشد المحوري مناسبة لتمثيل سلوك الشد المحوري لخلطات الخرسانة متفوقة الأداء.

INTRODUCTION

Research over the past decades has yielded Ultra High Performance Concrete (UHPC). It is a new generation of cement-based materials first developed in France in the 1990s. UHPC provides superior mechanical and durability properties compared to conventional and high performance concrete [1, 2]. This is because UHPC has several unique characteristics that set it apart from more conventional forms of concrete, including finer quartz aggregate, a lower water-to-cement ratio, and the presence of superplasticizers and fine ductile metal or polymer fibers [3]. The achievement of strain hardening behavior with strain capacities of more than 0.2% has been a challenge, particularly with UHPC matrices reinforced with short, smooth steel fibers. A large amount (V_f = 4-6%) of short, smooth steel fibers has been generally required to produce strain hardening behavior in UHPC matrices due to the relatively low bond strength of such fibers. The large amount of fiber significantly increases the cost of UHPFRC [4].

Due to its superior qualities, UHPFRC could be a suitable solution for structures, where high strength and durability properties are required. Since its first appearance, this material has been used in numerous structural applications in the field of bridges, pavements, and architectural structures. With the growing use of UHPFRC in modern construction, determining its tensile and compressive properties is essential in the study of its structural behavior, numerical modeling and fracture mechanics [5].

Many previous researches [6, 7, 8, 9, 10, 11] has been done to study the mechanical properties and the structural behavior of UHPC, but very little work has been done to investigate the behavior of UHPC under uniaxial direct tension, no detailed study has been found to propose a model for the uniaxial tensile behavior of UHPC.

EXPERIMENTAL PROGRAM

Materials:

Cement

Sulfate resisting Portland cement Type V was used throughout this research. Its chemical and physical properties conform to the provision of Iraqi specifications No.5 1984.

Fine Aggregate

AL-Ukhaider natural sand of maximum size 600μm was used. Its gradation lies in zone (4), as shown in Table (1). The gradation and sulfate content results of fine aggregate were within the requirements of the Iraqi specification No. 45/1980.

Admixtures

Two types of concrete admixtures were used in this work.

Superplasticizer

Superplasticizer of polycarboxylate ether polymer manufactured by PAC Technologies Company under the commercial name PC 200 was used to produce the UHPC mixes. This admixture complies with the requirements of ASTM C494.

Silica Fume

Silica fume has been used as a mineral admixture added to the UHPC mixes of this study. The percentages used were 10%, 15%, 20%, 25%, and 30% as partial replacement of cement weight. Its accelerated pozzolanic strength activity index with Portland cement at 7 days is 125.6%. The chemical composition and physical requirements show that the silica fume conforms to the chemical and physical requirements of ASTM C1240 specifications.

Steel Fibers

Hooked steel fibers used throughout the experimental program. The steel fiber used has diameter 0.5mm, length 30mm (aspect ratio $lf/\ df$ =60), density 7800 kg/m^3 and ultimate tensile strength of 1180 MPa.

Concrete Mixes

According to the features of UHPC mix design reported in previous researches[12-17], many mix proportions were tried in this investigation to have maximum compressive strength and flow of (110+5%) according to ASTM C109 and ASTM C1437 respectively. UHPC mixes are listed in Table (2). The variable parameters were, the silica fume content as partial replacement by weight of cement (0%, 10%, 15%, 20%, 25% and 30%) and steel fibers volume fraction as ratio of the mix volume (0%, 1%, 2% and 3%). All mixes shown in Table (2) had a flow ranging between 105% and 115%.

https://doi.org/10.30684/etj.33.1A.5
2412-0758/University of Technology-Iraq, Baghdad, Iraq

Mixing of Concrete

All UHPC mixes were performed in a rotary mixer of $0.1m^3$. For UHPC concrete, the silica fume and cement were mixed in dry state for about three minutes to disperse the silica fume particles throughout the cement particles, then the sand was added and the mixture was mixed for five minutes. The superplasticizer is dissolved in water and the solution of water and superplasticizer is gradually added during the mixing process then the whole mixture was mixed for 3 minutes. The mixer was stopped and mixing was continued manually especially for the portions not reached by the blades of the mixer. The mixer then operated for five minutes to attain reasonable fluidity. Fibers were uniformly distributed into the mix in 3 minutes, and then the mixing process continued for additional 2 minutes. In total, the mixing of one batch requires approximately 15 minutes from adding water to the mix.

Preparation and Testing of Specimens

All specimens were prepared, cured for 28 days then tested to study the uniaxial tensile behavior of UHPC. The uniaxial tensile test was performed on dogbone-shaped briquette (76 mm long, 25 mm thick, and 645-mm^2 cross section at mid-length) to determine the complete tensile stress-strain curve using a digital testing machine of 200 kN capacity with special self-aligning grips to allow for passive gripping of the specimen in the test machine and to ensure uniform loading.

The alignment of tensile set-up was carefully checked before testing and the specimens were installed with care to avoid any influence of eccentricity. At each value of the applied axial tensile load (P) from the load cell the corresponding tensile strain was measured using one electrical resistance strain gage attached at the mid-length of the specimen over a gauge length of 30 mm, as shown in Fig. (1).

Curing

All specimens were demolded after 24 hours, and then they were steam cured at about 90^oC for 48 hours in a water bath. After that they were left to be cooled at room temperature, and then they placed in water and left until the end of water curing at 28 days.

RESULTS AND DISCUSSION

Uniaxial Tensile Stress-Strain Relationship

Experimental Results

Figure (2) shows a typical uniaxial tensile stress-strain curve of UHPC specimens MFR0 and MFR1 (0% and 1% respectively). This typical curve starts with a steep initial ascending portion up to first cracking and it terminates at point (f_{te}, ε_{te}) showing no possible occurrence of strain hardening or multiple cracking and therefore a point with coordinates (f_{tp}, ε_{tp}) cannot be attained. The descending part of the tensile stress-strain curve was seen to vanish in specimen MFR0 while it showed a small tail in specimen MFR1.

The experimental results show that the uniaxial tensile stress-strain curves of the UHPC specimens MFR2 and MFR3 (containing fiber volume fraction V_f = 2% and 3% respectively) have a typical shape shown in Fig. (3). This typical curve starts with a steep initial ascending portion up to first cracking, followed by a strain-hardening branch where multiple cracking develops. The point where first cracking occurs is characterized by its stress and strain coordinates (f_{te}, ε_{te}); while the peak point at the end of the strain hardening branch is defined by the stress and strain (f_{tp}, ε_{tp}). At this peak point, one of the cracks widens up and becomes critical defining the onset of crack localization. Following the peak point, there is generally a descending branch describing the stage of fibers pull-out. The cement matrix may also contribute some tensile resistance along this part of the curve up to a certain crack opening.

The uniaxial tensile stress-strain curves of UHPC specimens with 0%, 1%, 2%, and 3% steel fibers are plotted in Fig. (4). Results indicated that the nonfibrous UHPC specimen (MFR0) and the specimen with steel fibers ratio 1% (MFR1) failed immediately after crack initiation, which occurred at a certain strain value and that once this strain value was exceeded, the load was found to decrease rapidly (strain softening behavior). Fibrous UHPC specimens with 2% and 3% steel fibers showed different tensile behavior. In these specimens the tensile failure was more ductile and gradual accompanied by the development of a main crack and many multiple secondary cracks.

The load was found to increase even after crack initiation (strain hardening behavior) and thereafter showed gradual declination. This behavior can be attributed to the ability of steel fibers to arrest and slow down the process of microcracks propagation. Figure (4) also shows that increasing the steel fibers volume fraction (V_f) from 0% to 3%, results not only in increasing the area under the uniaxial tensile stress–strain curves, but also increasing both the maximum uniaxial tensile strength by about 238.5% and its corresponding strain by about 4044%. This behavior can be attributed to the ability of steel fibers to bridge matrix crack and apply a closing pressure at the crack front. This reduces the stress-intensity at the crack tip, and a higher energy input is needed to further extend the crack. The amount of additional energy needed for crack extension depends mainly upon the physical and material properties of the fibers, and the properties of the matrix [18].

The uniaxial tensile stress-strain curves of UHPC specimens with silica fume content of 0%, 10%, 15%, 20%, 25%, and 30% are plotted in Fig. (5). This Figure shows that when silica fume content increased from 0% to 10%, 15%, 20%, 25%, and 30% the uniaxial tensile strength (f_{tp}) slightly increased by 2.63%, 3.96%, 9.5%, 14.04% and 16.89% respectively, but it shows no clear effect on the value of its corresponding strain (ε_{tp}) as shown in Table (3). This behavior can be attributed to the fact that the influence of silica fume addition has a reverse effect on toughness of UHPC.

The addition of silica fume makes the concrete denser and more brittle, accordingly, silica fume concrete will have lower toughness and less ability to gain more strain under excessive stresses. On the other hand, incorporation of silica fume will effectively enhance the fiber–matrix interfacial properties due to densification of the mix by the effect of microfilling and pozzolanic reaction of silica fume which increases the bond between the matrix and the fibers, therefore, the pullout energy is remarkably enhanced

[18,19]. Tension failure of UHPC briquettes with and without steel fibers is shown in Fig. (6). The experimental tensile stress-strain curves for all UHPC mixes of the present research are plotted in Fig. (7) to (15) and the coordinates of their maximum points are listed in Table (3).

Model for the Complete Uniaxial Tensile Stress-Strain Relationship of UHPC

Based on the results of the present experimental tests, a regression analysis is carried out using Data Fit computer program to obtain a curve fitting model for expressing the complete uniaxial tensile stress-strain relationship of UHPC mixes. Two nonlinear equations are suggested (Eqs. 1 and 2) to model the complete uniaxial tensile stress-strain relationship for all the UHPC mixes of the present study. Eq. (1) models the ascending part of the relationship with coefficient of multiple determinations $R^2 = 0.993$, while Eq. (2) models the descending part of the f_t - ε_t relationship with $R^2 = 0.958$.

$$f_t = f_{td}\left[a\left(\frac{\varepsilon_t}{\varepsilon_{td}}\right)\right]^b \quad \ldots.(1)$$

where:

a = 0.860, b = 6.474×10^{-2}

$$f_t = f_{td} \times \left[\frac{a\left(\frac{\varepsilon_t}{\varepsilon_{td}}\right)^b}{c+\left(\frac{\varepsilon_t}{\varepsilon_{td}}\right)^d}\right] \quad \ldots.(2)$$

where:

a = 169.259, b = -0.404

c = 164.580, d = 3.11

f_t : uniaxial tensile stress of concrete, MPa

ε_t : uniaxial tensile strain of concrete

f_{td} , ε_{td} : direct tensile strength (MPa) and its corresponding strain, which is f_{te} , ε_{te} for UHPC with strain softening behavior and f_{tp} , ε_{tp} for UHPC with strain hardening behavior.

Figures (7) to (15) show plots of the test results and the proposed model for the prediction of the uniaxial tensile stress- strain relationships of UHPC mixes investigated in the present study. The comparison between the experimental and proposed curves (as can be seen from these figures) show a very close agreement and therefore equations (1) and (2) can be considered as good representative equations for predicting the uniaxial

tensile behavior of UHPC mixes investigated in this study, and consequently may be useful to structural engineers in their design of reinforced UHPC structures.

Relationships between First Cracking Uniaxial Tensile Strength, Post Cracking Uniaxial Tensile Strength, and Their Corresponding Strain

A Data Fit computer program has been adopted to carry out a regression analysis for the sake of establishing an empirical equation to predict the relationship between the first cracking uniaxial tensile strength f_{te} and the post cracking uniaxial tensile strength f_{tp} for the ten UHPC mixes investigated in the present study with $R^2 = 0.967$ as given below.

$$f_{te} = 0.509 (f_{tp}) + 1.273 (V_f) \quad \text{....(3)}$$

where:
f_{te} : first cracking uniaxial tensile strength (MPa).
f_{tp} : post cracking uniaxial tensile strength (MPa).
V_f : steel fibers volumetric ratio.

Figure (16 **a**) shows the first cracking uniaxial tensile strength obtained from the experimental work (observed) versus the corresponding calculated strength using Eq. (3) (predicted), while Fig. (17 **b**) shows the ratio $f_{te\ observed} / f_{te\ predicted}$ versus the post cracking uniaxial tensile strength f_{tp}.

In the present study, two more empirical equations have also been suggested. Equation (4) is for predicting the first cracking uniaxial tensile strain with $R^2 = 0.955$ (as shown in Fig. 17); and Equation (5) is for predicting the post cracking uniaxial tensile strain with $R^2 = 0.97$ (as shown in Fig. 18).

$$\varepsilon_{te} = 2.17*10^{-5} (f_{te}) + 1.75*10^{-5} \quad \text{....(4)}$$

$$\varepsilon_{tp} = 2.47*10^{-4} (f_{tp}) + 6.74*10^{-} \quad \text{.... (5)}$$

where:
ε_{te} : first cracking uniaxial tensile strain.
ε_{tp} : post cracking uniaxial tensile strain.
f_{te} : first cracking uniaxial tensile strength (MPa).
f_{tp} : post cracking uniaxial tensile strength (MPa).

Evaluation of the Proposed Uniaxial Tensile Stress–Strain Response Equations

The accuracy of Equations (1) and (2) can be examined through the comparison between the uniaxial tensile stress–strain curves predicted by applying these two equations and the experimental uniaxial tensile stress–strain curves obtained by other investigators like Wille et al. [20] and Park et al. [4].

Wille et al. [20] studied the strain hardening of ultra high performance fiber reinforced concrete with compressive strength 192 MPa under direct tensile loading. Four types of

steel fibers were used including straight smooth, hooked, high twisted and low twisted steel fibers. Since the steel fibers used in this investigation is hooked, so the proposed model [Eqs.(1) and (2)] compared with the experimental results for concrete mixes containing hooked steel fibers only(with fiber content 1%, 1.5% and 2%) as shown in Fig.(19). The comparison between the proposed equations and the test results shows a good agreement.

Park et al. [4] investigated the effect of blending fibers on the tensile behavior of Ultra High Performance Hybrid Fiber Reinforced Concrete (UHP-HFRC) with compressive strength 200 MPa. Four types of steel macro- fibers (of different length or geometry) and one type of micro steel fiber were considered. Figure (20) shows the comparison between the proposed equations and the test results for UHP-HFRC containing 1% macro- steel fiber with different geometry (twisted, hooked and straight) and 1.5% micro-straight steel fiber. It can be observed that there is a slight deviation between the experimental results and the proposed results; this may be attributed to the different tensile behavior between mono (single) type fiber used in this investigation and hybrid fibers used by Park et al.

CONCLUSIONS

From the experimental results presented in this study, the following conclusions can be drawn:

1.The uniaxial tensile stress-strain relationship for different UHPC mixes indicated that the nonfibrous UHPC specimen and specimens with 1% steel fibers ratio failed (under direct tension) immediately after crack initiation which occurred at a certain strain value beyond which the stress decreased with increasing strain (strain softening behavior).

2.The brittle nature of failure was seen to change into a ductile failure in UHPC specimens containing 2% and 3% steel fibers ratio. These specimens failed by gradual development of main crack and many multiple cracks and the tensile stress increased even after crack initiation (strain hardening behavior) until peak stress value was reached and thereafter decreased gradually.

3.The increase in the steel fibers ratio from 0% to 3% did not only cause an increase in the area under the uniaxial tensile stress–strain curve, but also resulted in increase in the maximum uniaxial tensile strength and its relevant strain (ε_o) by about 238.5% and 4044% respectively.

4.The increase of silica fume content for UHPC mix with fiber content 2% caused a slight increase in the post cracking uniaxial tensile strength (f_{tp}) with no clear effect on its relevant strain (ε_{tp}).

5.Two nonlinear equations were suggested for modeling the complete uniaxial tensile stress-strain relationship of UHPC mixes of the present study. The first equation was for the ascending part of the relationship, while the second equation was for the descending part. The proposed equations showed a good agreement with the experimental results and can theoretically be used for predicting the uniaxial tensile behavior of UHPC.

Table (1) Fine aggregate properties

Sieve size (mm)	**Cumulative passing %**	**Limits of Iraqi specification No.45/1984, zone 4**
4.75	100	95-100
2.36	100	95-100
1.18	100	90-100
0.60	100	80-100
0.30	44	15-50
0.15	7	0-15
Fineness modulus = 1.5		
Specific gravity =2.69		
Sulfate content =0.13% (Iraqi specification requirement ≤ 0.5%)		
Absorption = 0.73%		
Material finer than 75μm=1.24%		

Group	Mix symbol	cement kg/m^3	fine sand kg/m^3	silica fume* (%)	silica fume kg/m^3	steel fibers** (%)	steel fibers content kg/m^3	w/cm ratio	HRWRA*** (%)	HRWRA type

Table (2) UHPC mixes used in the present research

1	MSP-P	935	1100	15%	165	2%	156	0.16	8.7%	PC200
2	MSF0	1100	1100	0%	0	2%	156	0.16	8.7%	PC20
	MSF10	990	1100	10%	110	2%	156	0.16	8.7%	PC20
	MSF15†	935	1100	15%	165	2%	156	0.16	8.7%	PC20
	MSF20	880	1100	20%	220	2%	156	0.17	8.7%	PC20
	MSF25††	825	1100	25%	275	2%	156	0.18	8.7%	PC20
	MSF30	770	1100	30%	330	2%	156	0.18	8.7%	PC20
3	MFR0	825	1100	25%	275	0%	0	0.17	8.7%	PC20
	MFR1	825	1100	25%	275	1%	78	0.17	8.7%	PC20
	MFR2	825	1100	25%	275	2%	156	0.18	8.7%	PC20
	MFR3	825	1100	25%	275	3%	234	0.187	8.7%	PC200

MSF15 in group 2 is the same mix designated MSP-P in group 1
MSF25 in group 2 is the same mix designated MFR2 in group 3
Percent by weight of cement.
Percent of mix volume.
Percent of cementitious materials (cement + silica fume) weight.

Figure (1) Tests set-up

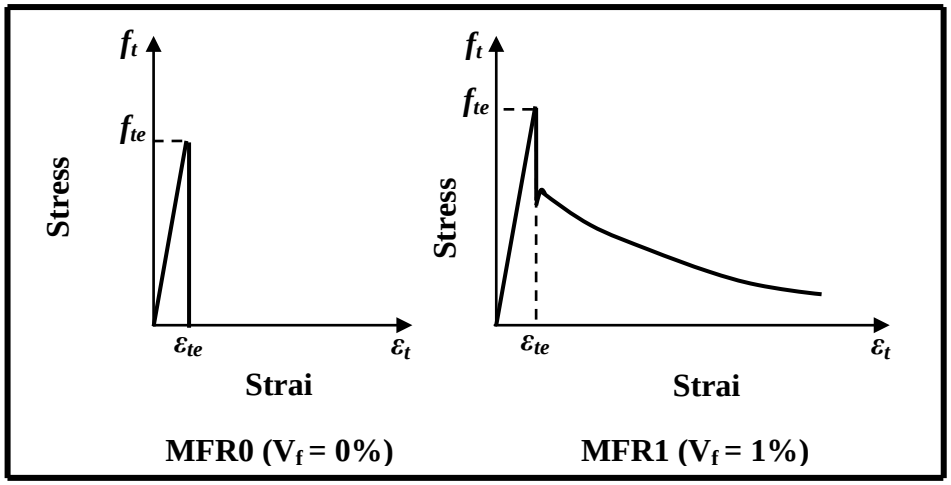

Figure (2): Uniaxial Tensile stress-strain curve of UHPC with strain softening behavior

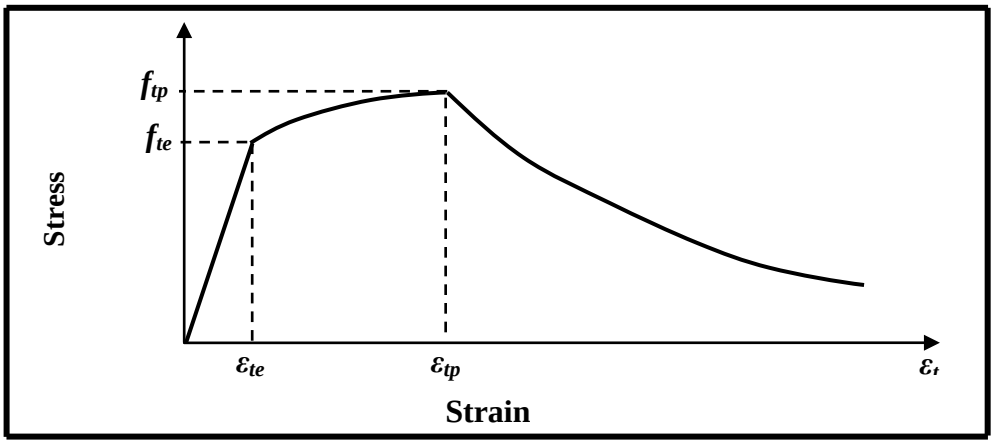

Figure (3): Uniaxial Tensile stress-strain curve of UHPC with strain hardening behavior

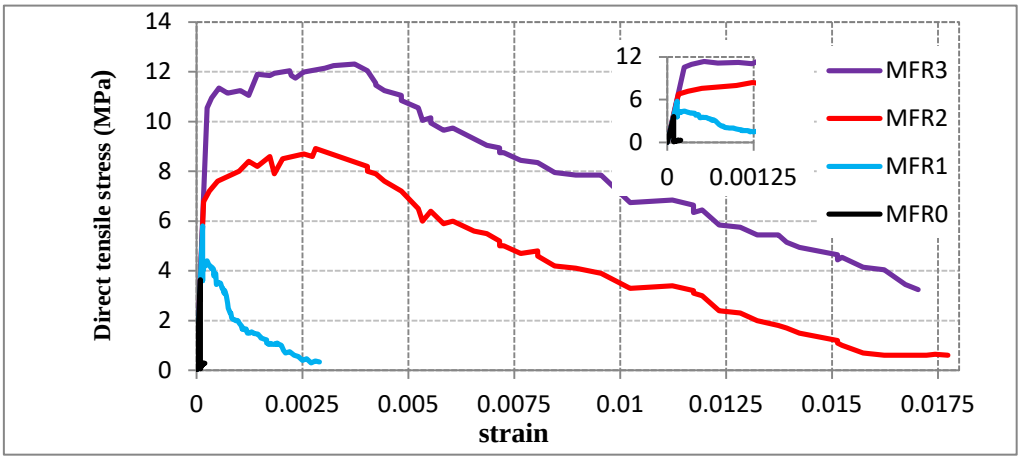

Figure (4) Effect of steel fibers volume fraction (V_f) on the uniaxial tensile stress-strain relationship of UHPC

Group	Mix Symbol	Silica Fume SF (%)	Steel fibers V_f (%)	f_{te} (MPa)	f_{tp} (MPa)	ε_{te}	ε_{tp}	f_{te}/f_{tp} (%)

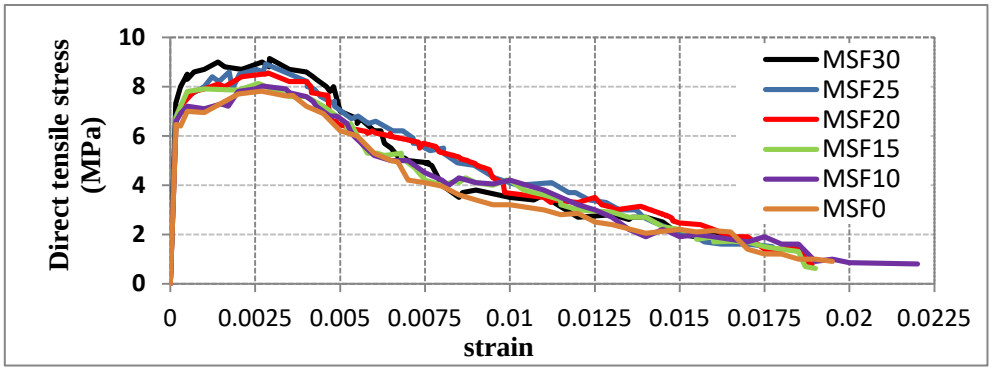

1	**MSP-P**	15%	2%	6.74	8.13	0.000164	0.00259	82.91
2	**MSF0**	0%	2%	6.47	7.82	0.000170	0.00268	82.75
	MSF10	10%	2%	6.59	8.03	0.000169	0.00271	82.12
	MSF15	15%	2%	6.74	8.13	0.000164	0.00259	82.91
	MSF20	20%	2%	6.68	8.56	0.000168	0.00287	78.02
	MSF25	25%	2%	6.78	8.92	0.000162	0.00281	76.01
	MSF30	30%	2%	7.32	9.14	0.000161	0.00292	80.09
3	**MFR0**	25%	0%	3.64	-	0.00009	-	-
	MFR1	25%	1%	5.80	-	0.000141	-	-
	MFR2	25%	2%	6.78	8.92	0.000162	0.00281	76.01
	MFR3	25%	3%	10.55	12.32	0.000245	0.00373	85.63

Figure (5) Effect of silica fume content on the uniaxial tensile stress-strain relationship of UHPC

Table (3): Tensile properties of UHPC mixes

UHPC with steel fibers UHPC without steel fibers

Figure (6) Tension failure of UHPC briquettes with and without steel fibers

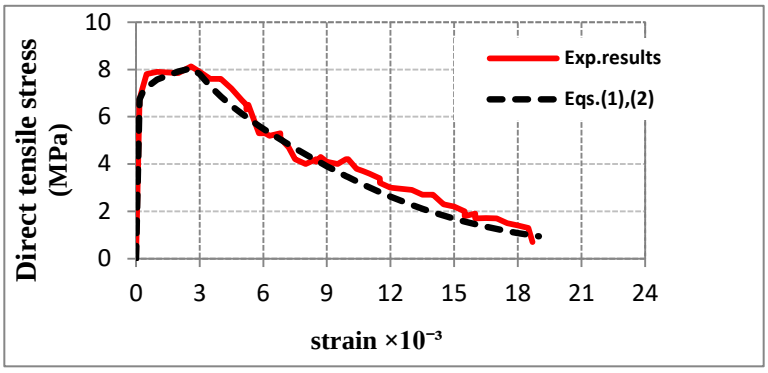

Figure (7) Tensile stress-strain curves for (MSP-P) mix

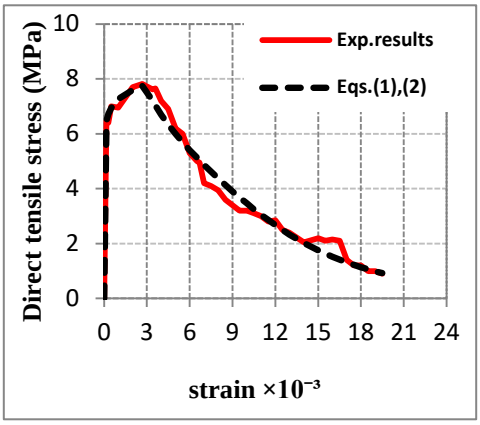

Figure (8) Tensile stress-strain curves for (MSF0) mix

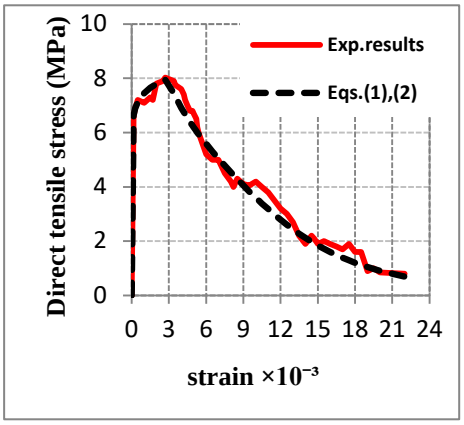

Figure (9) Tensile stress-strain curves for (MSF10) mix

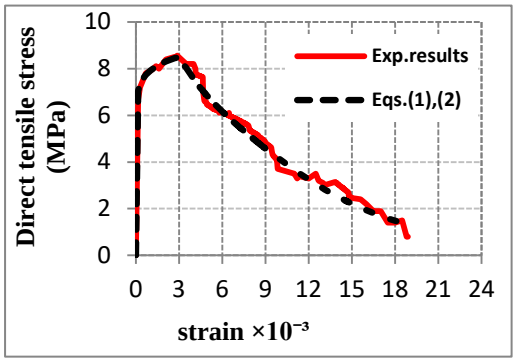

Figure (10) Tensile stress-strain curve curves for (MSF20) mix

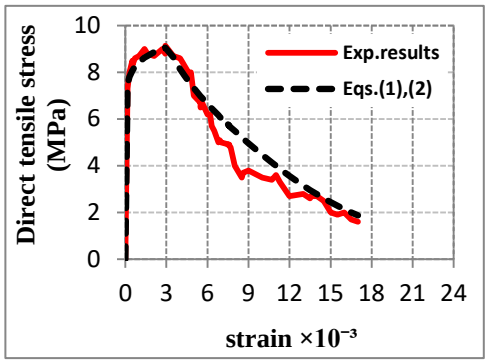

Figure (11) Tensile stress-strain for (MSF30) mix

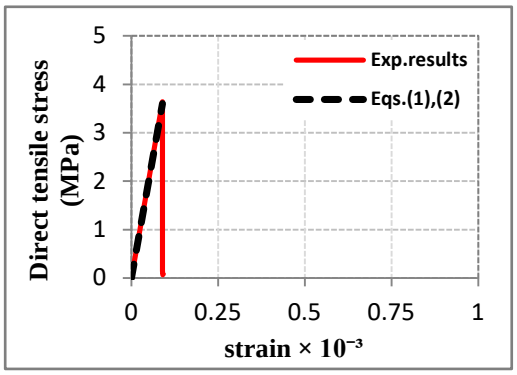

Figure(12) Tensile stress-strain curves curves for (MFR0) mix

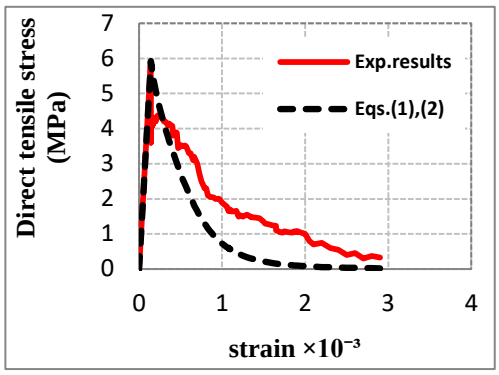

Figure (13) Tensile stress-strain for (MFR1) mix

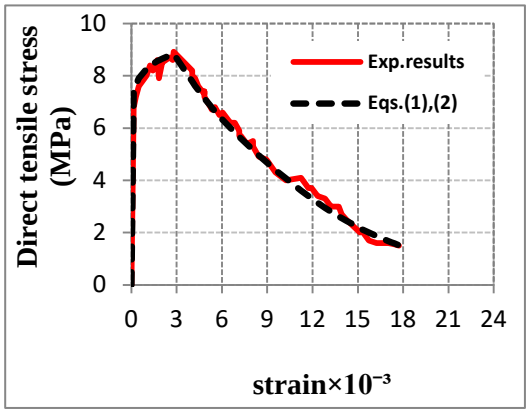

Figure (14) Tensile stress-strain curves for (MFR2) mix

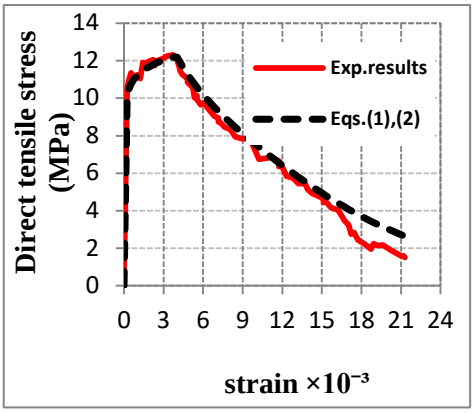

Figure(15) Tensile stress-strain curves for (MFR3) mix

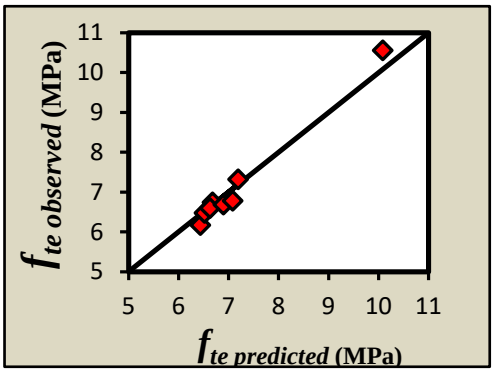

(a)

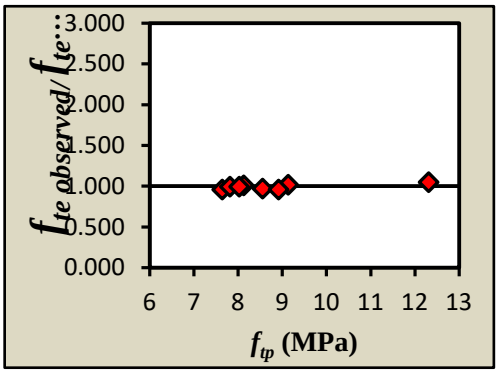

(b)

Figure (16) (a) Observed versus predicted values of first cracking uniaxial tensile strength, (b) The ratio $f_{te\ observed}$ / $f_{te\ predicted}$ versus the post cracking uniaxial tensile strength f_{tp}

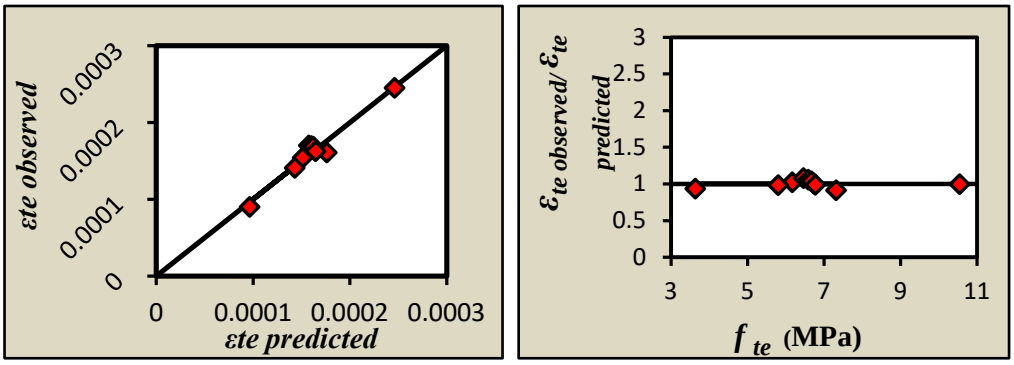

(a) **(b)**

Figure(17) (a) Observed versus predicted values of first cracking uniaxial tensile strain, (b) The ratio $\varepsilon_{te\ observed}$ / $\varepsilon_{te\ predicted}$ versus the first cracking uniaxial tensile strength f_{te}

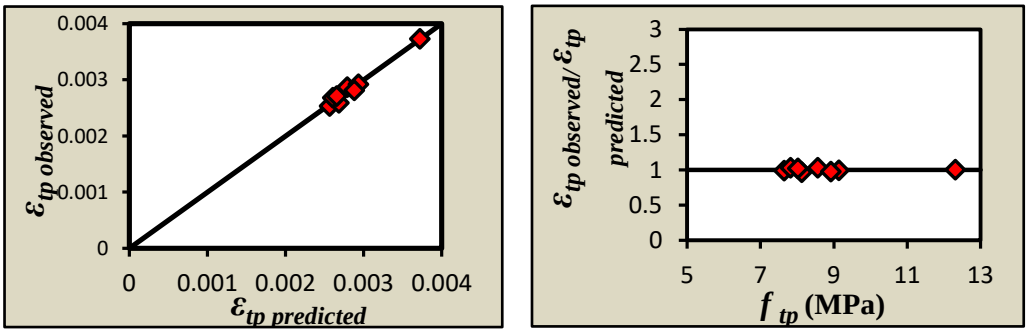

(a) **(b)**

Fiure. (18) (a) Observed versus predicted values of post cracking uniaxial tensile strain, (b) The ratio $\varepsilon_{tp\ observed}$ / $\varepsilon_{tp\ predicted}$ versus the post cracking uniaxial tensile strength f_{tp}

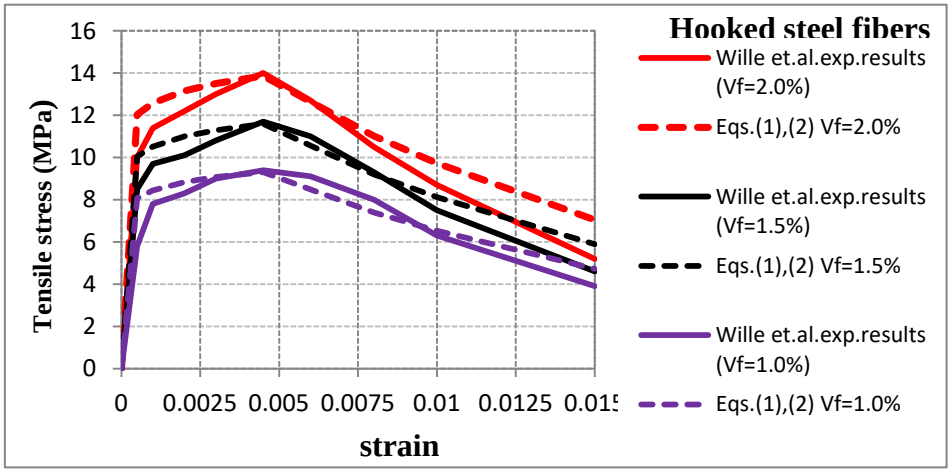

Figure (19): Comparison between the experimental and proposed uniaxial tensile stress-strain curves of UHPC with hooked steel fibers

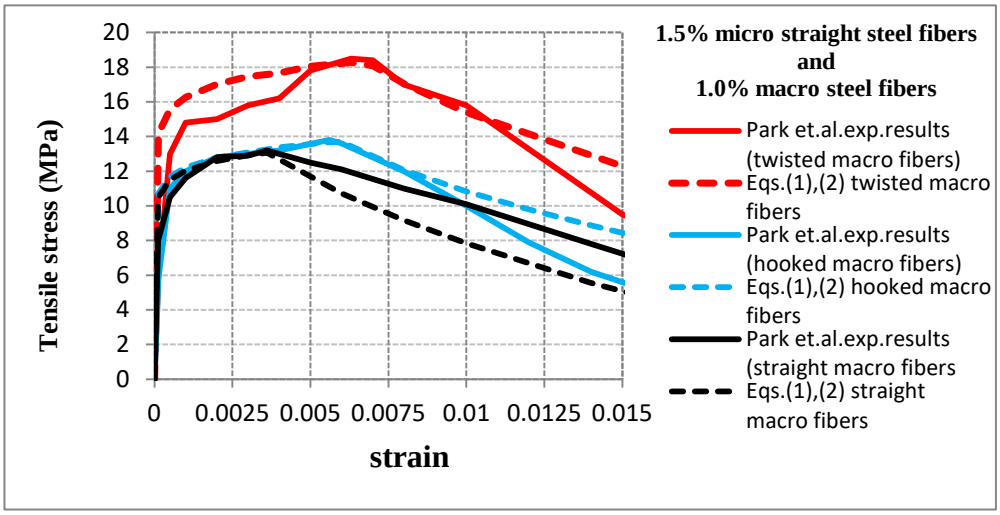

Figure (20): Comparison between the experimental and proposed uniaxial tensile stress-strain curves of UHPC with 1.5% micro steel fibers and 1.0% macro steel fibers according to the types of macro fiber

REFERENCE

[1].Richard, P., and Cheyrezy, M. H., "Reactive Powder Concretes with High Ductility and 200-800 N/mm2 Compressive Strength", ACI Special Publication, Vol. 144, No. 24, 1994, pp. 507-518.

[2].Azad, A. K., and Ahmad, S., "Effect of Cyclic Exposure and Fiber Content on Tensile Properties of Ultra- High Performance Concrete", Advances in cement Research, Vol. 25, Issue 5, 2013, pp. 273-280.

[3].Buck, J. J., McDowell, D. L., and Zhou, M., "Effect of microstructure on load-carrying and energy-dissipation capacities of UHPC", Cement & Concrete Research, Vol. 43, 2013, pp. 34–50.

www.ivsl.org

[4].Park, S. H., Kim, D. J., Ryu, G. S., and Koh, K. T., "Tensile Behavior of Ultra High Performance Hybrid Fiber Reinforced Concrete", Cement & Concrete Composites, Vol. 34, No. 2, 2012, pp. 172–184.

www.ivsl.org

[5].Hassan, A. M. T., Jones, S. W., and Mahmud, G. H., "Experimental test methods to determine the uniaxial tensile and compressive behaviour of ultra high performance fibre

reinforced concrete (UHPFRC)", Construction and Building Materials, Vol. 37, 2012, pp. 874–882.

www.ivsl.org

[6]. Kange, S. T., Park, J. J., Ryu, G. S., Koh, G. T., and Kim, S. W., "Comparison of Tensile Strengths with Different Test Methods in Ultra High Strength Steel-Fiber Reinforced Concrete (UHS-SFRC)" , key Engineering Materials, Vols. 417-418, 2010, pp.649-652.

[7]. Dirk, W., and Jianxin, M., "Mechanical Properties of Ultra High Strength Concrete", University of Leipzig, LACER No. 8, 2003, pp. 175-184.

[8] Yang, I. H., Joh, C., and Kim, B., "Structural Behavior of Ultra High Performance Concrete Beams Subjected to Bending", Engineering Structures, Vol. 32, No. 11, 2010, pp. 3478–3487.

[9]. Kim, D. J., Park, S. H., Ryu, G. S., and Koh, K. T., "Comparative Flexural Behavior of Hybrid Ultra High Performance Fiber Reinforced Concrete with Different Macro Fibers", Construction and Building Materials, Vol. 25, No. 11, 2011, pp. 4144–4155.

[10]. Kang, S. T., Lee, B. Y., Kim, J. K., and Kim, Y. Y., "The Effect of Fiber Distribution Characteristics on the Flexural Strength of Steel Fiber-Reinforced Ultra High Strength Concrete", Construction and Building Materials, Vol. 25, No.5, 2011, pp. 2450–2457.

[11]. Al- Hassani, H. M., Khalil, W. I., and Danha, L. S., " Mechanical Properties of Reactive Powder Concrete (RPC) with Various Steel Fiber and Silica Fume Content", Engineering and Technology Journal, Vol.31, Part (A), No.16, 2013.

[12]. Sobolev, K., and Soboleva, S., "Properties of Ultra High Strength Cement", Civil Engineering Department, European University of Lefke, Turkey, pp. 1-15.

[13]. Gao, R., Stroeven, P., and Hendriks, C. F., "Mechanical Properties of Reactive Powder Concrete Beams", ACI Special Publication, Vol. 228, No. 79, 2005, pp.1237-1252.

[14]. Dauriac, C. "Special Concrete May Give Steel Stiff Competition", The Seattle Daily Journal of Commerce, May 9, 1997, p.5.

[15]. Voo, J., Foster, S., and Gilbert, R., "Shear Strength of Fiber Reinforced Reactive Powder Concrete Girders without Stirrups", the University of New South Wales, Sydney 2052 Australia, UNICIV Report No. R-421 November 2003, p.131.

[16]. Orgass, M. and Klug, Y., "Steel Fiber Reinforced Ultra High Strength Concretes", Institute for Structural Concrete and Building Materials, University of Leipzig, MFPA Leipzig GmbH, Lacer No. 9, 2004, p.12.

[17]. Al-Ne'aime, S. S., "Static and Impact Properties of Reactive Powder Concrete", Ph.D. Thesis, University of Technology, Baghdad, 2006, p.190.

[18]. Dubey, A., and Banthia, N., "Influence of High-Reactivity Metakaolin and Silica Fume on the Flexural Toughness of High-Performance Steel Fiber-Reinforced Concrete", ACI Materials Journal, Vol. 95, No.3, 1998, pp. 284-292.

[19]. Chan, Y., and Chu, S., "Effect of Silica Fume on Steel Fiber Bond Characteristics in Reactive Powder Concrete", Cement and Concrete Research, Vol. 34, No. 7, 2004, pp. 1167–1172.

[20]. Wille, K., Kim, D. J., Naaman, A. E., "Strain-Hardening UHP-FRC with Low Fiber Contents", Materials and Structures, Vol. 44, No.3, 2011, pp. 583–598.